ESRF	**Experiment title:** Spin states of Co ions in cobaltites studied by spin selective resonant X-ray scattering spectroscopy near the Co *K* absorption edge	**Experiment number**: HC 2890
Beamline: MB20	**Date of experiment**: from: 18.10.2016 to: 23.10.2016	**Date of report**: 08-02-2017
Shifts: 15	**Local contact(s)**: Dr. Kristina Kvashnina	*Received at ESRF:*

Names and affiliations of applicants (* indicates experimentalists):

Vitaly V. Mesilov*, Vadim R. Galakhov*, M. N. Miheev Institute of Metal Physics, Ural Branch of RAS, 620137 Yekaterinburg, Russia

Margarita S. Udintseva*, Ural State University of Railway Transport, 620134 Yekaterinburg, Russia

Report:

Layered cobalt oxide compounds $LnBaCo_2O_{5+x}$ (where Ln — rare earth cation) have a perovskite-derived structure. Theses materials are characterized by unusual magnetic and electric transport properties [1,2]. Cobalt cations can exist in different oxidation and spin states. With an ideal oxygen stoichiometry of 5.5 per formula unit, the average oxidation state of Co is 3+. For Co^{3+} ions, high spin, low spin, and intermediate spin states are possible [3]. One can suggest that spin state transitions can be induced not only by changing temperature but also due to transfer of these materials into the nanostructured states. The transfer of single-crystalline or coarse-grain cobaltites containing Co^{3+} ions to the nanostructured state should lead to the $Co^{3+} \rightarrow Co^{2+}$ transition or to the appearance of low-spin instead of high-spin Co^{3+} ions.

Cobalt-doped anatase $Ti_{1-x}Co_xO_2$ nanopowders are characterized by ferromagnetic properties (see, for example, our work [4] and references therein). Therefore, an information concerning the valence state of cobalt impurity atoms is very important for understanding nature of ferromagnetism in these compounds.

We have studied the following systems: (i) nanostructured samples of $EuBaCo_2O_{5.5}$ and $TbBaCo_2O_{5.5}$ in which nanostates were obtained by milling and by shear deformation under pressure, respectively; (ii) cobalt-doped anatase $Ti_{1-x}Co_xO_2$ nanopowders; (iii) iron-doped anatase $Ti_{1-x}Fe_xO_2$ nanopowders; (iv) carbon encapsulated Fe@C nanoparticles. As reference compounds, pure Co and Fe metals, single crystalline CoO (Co^{2+} ions) and $LaCoO_3$ (Co^{3+} ions) samples were used.

The experiments were performed on the MB20 beamline. XAS spectra were simultaneously measured both in total fluorescence yield (TFY) mode and in high-energy-resolution fluorescence detected (HERFD) mode. Co *K*β and Fe *K*β X-ray emission spectra were measured in normal and resonant modes. Resonant

---

[1] A. A. Taskin, A. N. Lavrov, and Yoichi Ando. Transport and magnetic properties of $GdBaCo_2O_{5+x}$ single crystals: A cobalt oxide with square-lattice CoO_2 planes over a wide range of electron and hole doping. Phys. Rev. B 71, 134414 (2005).

[2] K. Conder, A. Podlesnyak, E. Pomjakushina, and M. Stingaciu. Layered cobaltites: Synthesis, oxygen nonstoichiometry, transport and magnetic properties. Acta Physica Polonica A 111, 7–14 (2007).

[3] M. A. Korotin, S. Yu. Ezhov, I. V. Solovyev, et al. Intermediate-spin state and properties of $LaCoO_3$. Phys. Rev. B 54, 5309−5326 (1996).

[4] A. Ye. Yermakov G. S. Zakharova, M. A. Uimin, et al. Surface magnetism of cobalt-doped anatase TiO_2 nanopowders. J. Phys. Chem. C 120, 28857−28866 (2016).

inelastic X-ray scattering (RIXS) spectra were obtained too. Some XES measurements were carried out at temperature of 100 K.

In Fig. 1, Co *K* X-ray absorption spectra (in HERFD mode) of a $LaCoO_3$ single crystal and $EuBaCo_2O_{5.5}$ and $TbBaCo_2O_{5.5}$ ceramics in the initial and nanostructured states are presented. Nanostructured powder of $EuBaCo_2O_{5.5}$ was obtained by milling the initial coarse-grained powder in a ball mill for 9 h [5]. The nanostructured state of $TbBaCo_2O_{5.5}$ was obtained by shear deformation under pressure of 7 GPa with the rotation angle of one anvil with respect to another equal to 180° [6]. The lack of a Co *K* edge shift indicates that the Co valence state remains unchanged (3+). The prepeak at about 7710 eV mainly reflects the density of empty Co 3*d* orbitals hybridizated with oxygen 2*p* orbitals. One can suggest that the lowest unoccupied states in $EuBaCo_2O_{5.5}$ and $TbBaCo_2O_{5.5}$ correspond to the t_{2g} states.

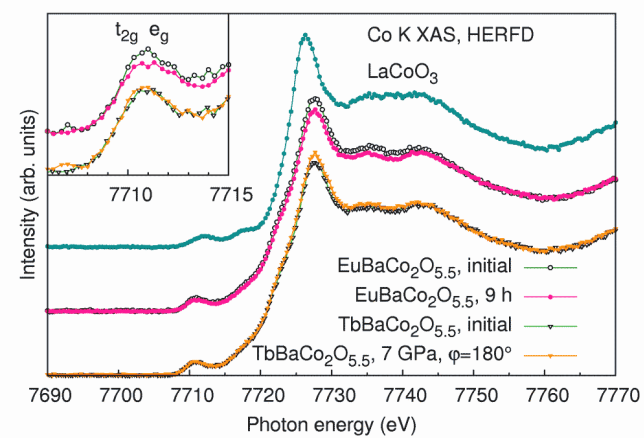

Fig. 1. Co *K* X-ray absorption spectra of a single crystal of $LaCoO_3$, $EuBaCo_2O_{5.5}$ in the initial state and after milling for 9 h, $TbBaCo_2O_{5.5}$ in the initial state and in the nanostructured state obtained by shear deformation under pressure of 7 GPa with the rotation angle of one anvil with respect to another equal to 180°. The spectra were measured in HERFD mode.

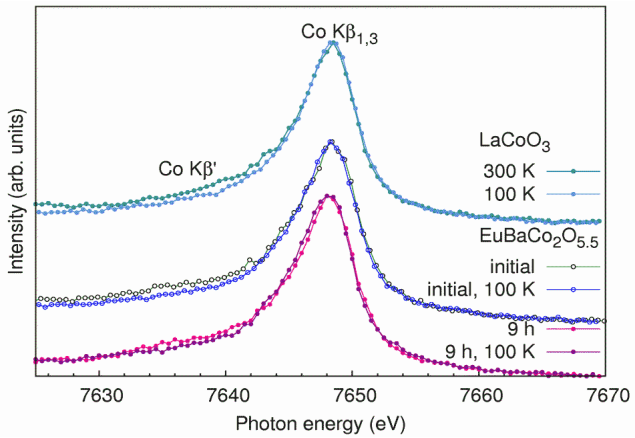

Fig. 2. Co $K\beta_{1,3}$ X-ray emission spectra of $LaCoO_3$ and $EuBaCo_2O_{5.5}$ in the initial state and after milling for 9 h. The spectra were measured at room temperature (300 K) and at temperature of about 100 K.

Fig. 2 shows Co $K\beta_{1,3}$ X-ray emission spectra of $LaCoO_3$ and $EuBaCo_2O_{5.5}$ in the initial state and after milling for 9 h. The spectra were measured at room temperature (300 K) and at temperature of about 100 K. The spectra measured at 100 K are characterized by the low $K\beta'$ satellite intensity in comparison with the spectra measured at room temperature. It means that a transition of a small part of high-spin Co^{3+} ions to the low-spin state occurred at low temperatures.

Fig. 3 shows RIXS spectra of $EuBaCo_2O_{5.5}$ in the initial state (a) and after milling for 9 h (b). RIXS data are shown here as a contour map in a plane of incident and transferred photon energies, where the vertical axis represents the energy difference between the incident and emitted energies. The spectra appeared to be closely allied. No extra structure in the pre-edge region was found. Therefore, the oxidation state of Co ions in these samples is the same: 3+.

In Fig. 4, Co *K* X-ray absorption spectra (in HERFD mode) of $Ti_{0.96}Co_{0.04}O_2$ nanopowders in the as-prepared state, after annealing at 700 °C in vacuum or in hydrogen are shown. For comparison, the spectra of Co metal and CoO are presented. The spectra of the samples after heating are similar but differ from the spectrum of the as-prepared sample.

Fig. 5 shows the experimental Co $K\beta$ RIXS energy loss maps over the pre-edge region of $Ti_{0.96}Co_{0.04}O_2$ nanopowders in the as-prepared state, after annealing at 700 °C in vacuum or in hydrogen. Note, in the work [7], Co $K\beta$ RIXS spectra measured on CoO shows an extra-energy-loss feature at about 62 eV for

---

[5] V. R. Galakhov, V. V. Mesilov, S. N. Shamin, et al. X-ray spectra and valence states of cations in nanostructured half-doped $La_{0.5}Ca_{0.5}MnO_3$ manganite. Appl. Phys. A 118, 649–654 (2015).

[6] V. V. Mesilov, V. R. Galakhov, B. A. Gizhevskii, et al. Application of X-ray absorption spectroscopy to the investigation of charge states of iron ions in iron borate nanoceramics. Phys. Solid State 56, 282–286 (2014).

[7] M. Al Samarai, M. U. Delgado-Jaime, H. Ishii et al. 1*s*3*p* resonant inelastic X-ray scattering of cobalt oxides and sulfides. J. Phys. Chem. C 120, 24063–24069 (2016).

the incident energy of 7709 eV. Our measurements carried out on a single crystal of CoO and $Ti_{0.96}Co_{0.04}O_2$ nanopowders did not show extra features in the RIXS spectra.

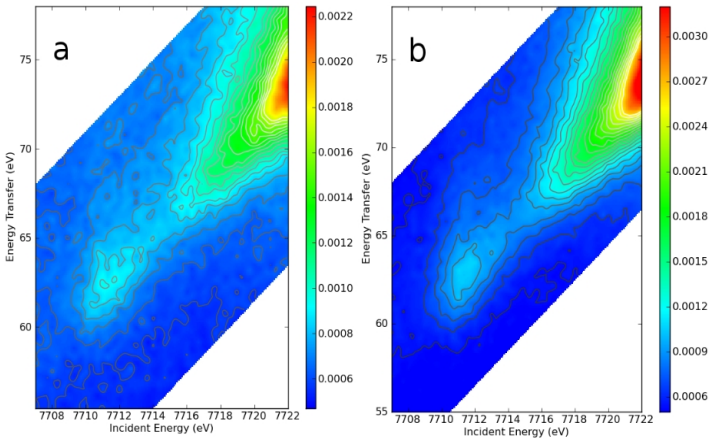

Fig. 3. Co *K*β RIXS energy-loss maps over the pre-edge region of $EuBaCo_2O_{5.5}$ in the initial state (a) and after milling for 9 h (b).

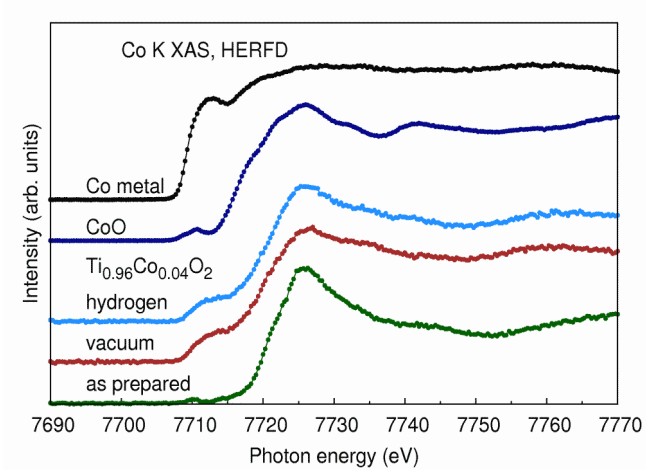

Fig. 4. Co *K* X-ray absorption spectra of $Ti_{0.96}Co_{0.04}O_2$ nanopowders in the as-prepared state, after annealing at 700 °C in vacuum or in hydrogen. Spectra of Co metal and CoO (single crystal) are shown too.

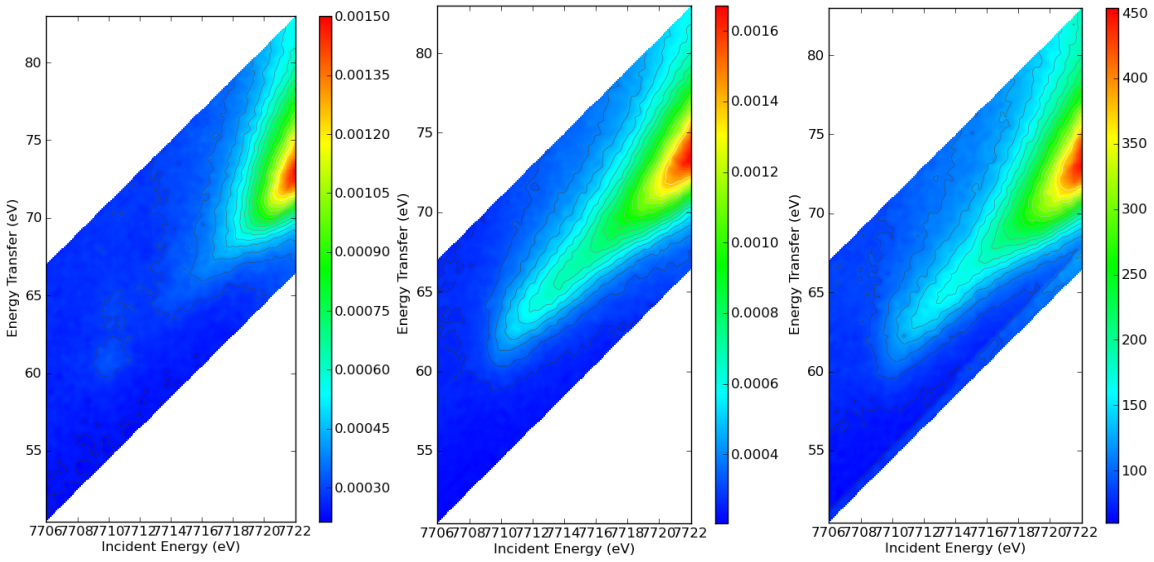

Fig. 5. Co *K*β RIXS energy-loss maps over the pre-edge region of $Ti_{0.96}Co_{0.04}O_2$ nanopowders in the as-prepared state (left), after annealing at 700 °C in vacuum (center) or in hydrogen (right).

Future experiments suggest: (i) measurements of Co and Fe *K*β emission line at different temperatures (from about 10 K to 600 K); (ii) measurements of RIXS spectra in a large energy-loss interval in order to cover both *K*β lines with satellites.